Jahn-Teller effect on F centers in barium sulfide

Y. M. Kapoor* and E. B. Hensley
Department of Physics, University of Missouri, Columbia, Missouri 65211
(Received 20 March 1980; revised manuscript received 20 January 1981)

Crystals of BaS were grown and additively colored in Ba vapor. A broad F band was observed in the optical absorption spectra with three partially resolved peaks at 1.7, 2.33, and 2.75 eV. The shape of this band was found to be independent of the density of coloration, indicating that the band was due to transitions of a single center. Calculations of the shape of the F-center absorption were carried out using a nine-dimensional Monte Carlo integration. This procedure not only made possible the inclusion of all of the linear and quadratic terms in the interaction Hamiltonian but also the mixing of nondegenerate with degenerate excited states. Assuming an $s^2 \rightarrow sp$-type transition, a good fit to the experimental band shape was obtained based on the $^1P_1$-orbital triplet excited state being split by the Jahn-Teller interaction, primarily the E_g modes, and being perturbed by an $^1S_0$ excited state coupled by the T_{1u} modes. A luminescence was observed in the colored crystals but it was shown that no radiative transitions were to be expected from the $^1P_1$ excited state of the F center and that the luminescence observed was probably due to an unknown impurity.

I. INTRODUCTION

The study of color centers in solids has been dominated throughout most of its history by investigations involving the alkali halides. In recent years, investigations involving the alkaline-earth oxides[1] have revealed many interesting features of color centers not readily evident in the alkali halides. These investigations involving the alkaline-earth chalcogenides represent ideal extensions to those involving the alkali halides because of the similarity of their structures. Most of both families of crystals have the NaCl crystal structure and both are made of ions having rare-gas electronic configurations, the principal difference being that the ions in the alkaline-earth chalcogenides are divalent rather than monovalent. This not only leads to stronger interactions but also to a greater variety of centers. For example, anion vacancies may contain either one electron (F^+ centers) or two electrons (F centers). Also it should be noted that the two-electron F center has negligible spin-orbit coupling, greatly facilitating the analysis of the vibronic interactions in these centers. However, except for one paper on the ESR of the F^+ center in BaS,[2] nothing has been reported on the F centers in the alkaline-earth chalcogenides other than for the oxides.

In this investigation, F centers were introduced into BaS by additive coloration. The absorption spectra showed three partially resolved peaks, reminiscent of the F-center absorption in the cesium halides. This strongly suggested that the band was being split by the Jahn-Teller interaction.[3] The most obvious candidate for this Jahn-Teller interaction was the T_{2g} vibrational mode since it is the only active mode, that is, the only mode that can split the absorption band. However, we will show that such an explanation is incorrect and that the splitting arises due to the passively active E_g mode being perturbed by a nearby s-like state.

To analyze the shape of the F-center absorption band we will make use of a Monte Carlo integration technique first used by Cho[4] and extended here to include the quadratic terms in the interaction Hamiltonian and also the mixing of nondegenerate electronic states with degenerate states. It should be noted that both of these extensions are necessary in order to account for the observed shape of the F band in BaS but that neither can be taken into account when the Henry, Schnatterly, and Slichter method-of-moments analysis[5] is used without greatly complicating the analysis. In addition, we point out that the Monte Carlo technique does not require the Condon approximation in which the dependence of the electronic part of the Born-Oppenheimer wave functions on the nuclear coordinates is neglected. In fact, within the semiclassical approximation (static Jahn-Teller effect), the Monte Carlo method appears to be capable of handling any additions to the interaction Hamiltonian that can be explicitly written down, with no additional approximations and with only modest increases in computing time.

II. EXPERIMENTAL

Single crystals of BaS were grown using a plasma torch, tip fusion process similar to the Vernoulli process used for growing sapphires. The torch used was similar to one described by Read.[6] The principal modifications were a water jacket of fused quartz around the outer

tube and the powder feed was injected at the base of the torch. The gas used was a mixture of argon and nitrogen with about 5 vol.% hydrogen. The hydrogen was included in an attempt to reduce any oxides that form or might already be present. How successful this was is very difficult to evaluate. The crystal-growing chamber was sealed and filled with the inert or reducing gases from the torch.

The crystals[7] were additively colored at temperatures between 1250 and 1500°C in barium vapor at pressures from 0.001 to 0.1 Torr using techniques that have been previously described.[8] Similar to BaO, BaS was found to react with the tantalum coloring bombs and hence the crystals were protected by using an MgO enclosure.[9]

Optical-absorption measurements were made using a Cary model 14 spectrophotometer. The upper two curves in Fig. 1 show the optical absorbance of a heavily colored crystal at room temperature RT, and liquid-nitrogen temperature LNT. The absorbance was also obtained for liquid-helium temperature LHT, but was found to be essentially indistinguishable from that at LNT. Three partially resolved peaks can be seen in the absorption band. It was demonstrated that these three peaks are due to transitions in a single-type center and not, for example, due to the F, F^+ centers and an impurity, by comparing the spectra with that of a very lightly colored crystal. The bottom two curves in Fig. 1 are for a lightly colored crystal at LNT and a clear crystal that had been annealed but not colored. Both LNT curves were corrected for reflection and background (mostly the wing of the exciton) by subtracting the absorbance of the clear crystal. After normalizing to the same peak height, these were plotted as the middle two curves in Fig. 1. Within the experimental uncertainties, these two curves are identical. The ratios of the low-energy peak to the central peak and the high-energy peak to the central peak were measured for all 14 crystals colored. These crystals varied in density of color centers over a range of 35. The deviations of the above ratios from each other were less than 10%.

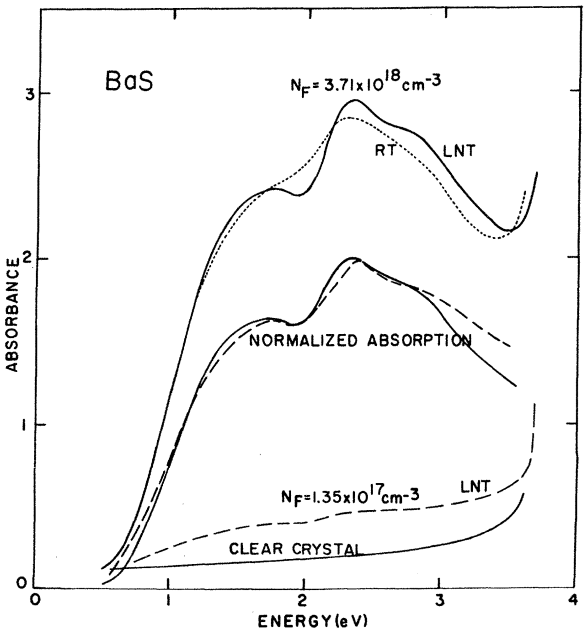

FIG. 1. Optical absorbance of F center in BaS. Upper two curves are for a heavily colored crystal measured at room temperature RT and liquid-nitrogen temperature LNT. Lower two curves are for a lightly colored crystal and an uncolored but annealed crystal, both at LNT. The center two curves are the optical absorptions for the two colored crystals at LNT normalized to the same height.

As a further check to make sure that two of the peaks in the observed spectrum were not due to both F and F^+ centers, an attempt was made to observe an $F \rightarrow F^+$ photoconversion. Such photoconversions have been observed for all of the alkaline-earth-oxide F centers. In spite of intensive efforts using high-intensity-light sources, no photoconversion could be seen for any of the three peaks. Thus all of our experimental observations pointed to the entire spectrum being due to a single-type center which we concluded was the F center.

Although it was not originally intended that a careful study of the mass-action law be made as was done for BaO,[9] sufficient data were obtained to make a useful estimate. The barium vapor pressure P_{Ba} was determined from the temperature at the bottom of the bomb T_{Ba}, using the practical vapor-pressure equations for barium developed by Nesmeyanov.[10] The density of Ba atoms at the crystal temperature T_c was then determined using the ideal-gas law $N_{Ba} = P_{Ba}/kT_C$. All optical-absorption data were taken at 77 K. The density of F centers was determined using Dexter's integral form of Smakula's equation.[11] The index of refraction for BaS was taken as 2.155 (Ref. 12) and the oscillator strength was arbitrarily chosen as 0.7. This resulted in the relation $N_F = 1.33 \times 10^{19} A_m/t$ where A_m is the absorbance at the central peak corrected for the clear crystal absorbance and t is the thickness of the crystal in mils.

Figure 2 shows a log-log plot of N_F vs N_{Ba}. The solid line is a least-squares fit to the equation $N_F^2 = 2.0 \times 10^{21} N_{Ba}$ for the 1522 K points. This implies that the centers are all singly ionized at the coloring temperature as was the case for BaO.[9] Also it will be noted that the higher-tem-

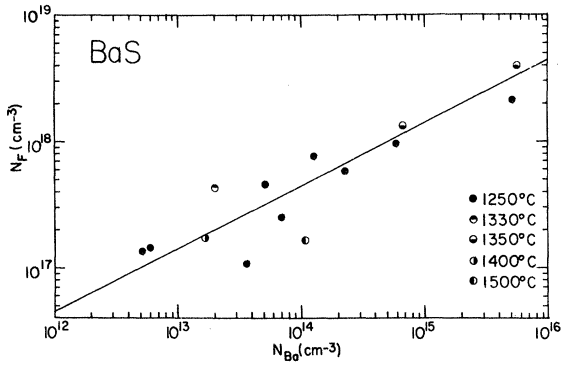

FIG. 2. Log-log plot of density of F centers N_F versus the density of Ba atoms in the vapor N_{Ba} for additive coloration. The straight line represents a least-squares fit of the 1250 °C points to the equation $N_F^2 = CN_{Ba}$.

perature points are distributed on both sides of this line, indicating that the temperature dependence of the constant in the above equation is less that the uncertainties in the measurements.

III. THEORY

The F center in BaS consists of two electrons trapped in an anion vacancy with transitions similar to those of the $s^2 \rightarrow sp$ transitions in the helium atom. It is improbable that the three peaks in the optical-absorption spectra can be attributed to the three allowed transitions $^1S_0$ $[^1A_{1g}] \rightarrow {}^1P_1[^1T_{1u}]$ (electric dipole allowed), $^1S_0$ $\rightarrow {}^3P_2[^3E_u$ and $^3T_{2u}]$ (vibration allowed), and $^1S_0$ $\rightarrow {}^3P_1[^3T_{1u}]$(spin orbit allowed) since the oscillator strengths would be expected to be radically different and the observed peaks have comparable intensities. On the other hand, the $^1P_1$ excited state is an orbital triplet whose degeneracy can be lifted by lattice vibrations similar to the splitting of the C bands in the alkali halides containing heavy-metal ions.[13] This is the Jahn-Teller interaction and is the basis of the analysis to be considered here.

The $^1P_1$ excited state of the F center in BaS has T_{1u} symmetry. In order for the interaction Hamiltonian to have nonvanishing matrix elements, the vibrational modes must have symmetries given by the symmetric product $[T_{1u} \times T_{1u}] = A_{1g} + E_g + T_{2g}$. Following Sturge,[14] the interaction coordinates will be designed Q_1 for A_{1g}, Q_2 and Q_3 for E_g, and Q_4, Q_5, and Q_6 for T_{2g}.

Calculations of the optical absorption of the F center as a function of the photon energy E were based on the equation

$$\mu(E) = \sum_f CA_\alpha E \int \cdots \int dQ_1 \cdots dQ_6 |\langle f|r|g\rangle|^2 \chi^*_{g\alpha}(Q_i)\chi_{g\alpha}(Q_i)\delta(E_f - E_{g\alpha} - E) \ , \tag{1}$$

where

$$C = (\mathcal{E}_{eff}/\mathcal{E}_0)^2(1/n)(4\pi^2e^2/3hc) \ .$$

The sum is over the three energy sheets of the excited state in $\vec{Q}$ space, $\mathcal{E}_{eff}$ is the magnitude of the electric field effective in inducing the transition, $\mathcal{E}_0$ is the average field in the medium, and n is the index of refraction. The symbol A_α indicates a statistical average over the occupied initial vibrational states, $\langle f|r|g\rangle$ is the dipole matrix element between the final and ground electronic states, and $\chi_{g\alpha}$ is the nuclear wave function of the ground state. Derivation of this equation follows the same reasoning used by Dexter[15] for his Eqs. (7.9) and (8.3), but modified to take into account lifting of the dengeneracy of the excited state. Specifically, the usual adiabatic or Born-Oppenheimer approximation and the Franck-Condon approximation were made. However, it will be noted that we do not make the Condon approximation in which the dependence of the electronic wave function on the nuclear coordinates is neglected but leave the dipole matrix elements inside the integral.[16] The interaction energies $E_{If}(Q_1 \cdots Q_6)$ and the electronic wave function

$$|f\rangle = a|x\rangle + b|y\rangle + c|z\rangle \tag{2}$$

are obtained by numerically diagonalizing the interaction Hamiltonian. The transition energies are given by

$$E_f(Q_1 \cdots Q_6) - E_g(Q_1 \cdots Q_6) = E_p + E_{If}(Q_1 \cdots Q_6) \ , \tag{3}$$

where E_p is the unperturbed transition energy to the p state.

Choosing $|x\rangle$, $|y\rangle$, $|z\rangle$ as the electronic basis functions for the excited state, the interaction Hamiltonian may be written

$$H_I = \begin{array}{c} \begin{matrix} |x\rangle & |y\rangle & |z\rangle \end{matrix} \\ \begin{bmatrix} h^1_{11}+h^q_{11} & h^1_{12}+h^q_{12} & h^1_{13}+h^q_{13} \\ h^1_{21}+h^q_{21} & h^1_{22}+h^q_{22} & h^1_{23}+h^q_{23} \\ h^1_{31}+h^q_{31} & h^1_{32}+h^q_{32} & h^1_{33}+h^q_{33} \end{bmatrix} \end{array} \ , \tag{4}$$

where the linear terms are

$$h^1_{11}=A_1Q_1/3^{1/2}-\tfrac{1}{2}B_1(Q_2-Q_3/3^{1/2}) ,$$
$$h^1_{22}=A_1Q_1/3^{1/2}+\tfrac{1}{2}B_1(Q_2+Q_3/3^{1/2}) ,$$
$$h^1_{33}=A_1Q_1/3^{1/2}-B_1Q_3/3^{1/2} ,$$
$$h^1_{12}=h^1_{21}=-C_1Q_6/6^{1/2} ,$$
$$h^1_{13}=h^1_{31}=-C_1Q_5/6^{1/2} ,$$
$$h^1_{23}=h^1_{32}=-C_1Q_4/6^{1/2} ,$$

and the quadratic terms are

$$h^q_{11}=A_{\alpha\alpha}\frac{1}{\sqrt{3}}Q_1^2+A_{\epsilon\epsilon}\frac{1}{\sqrt{6}}(Q_2^2+Q_3^2)+A_{\tau\tau}\tfrac{1}{3}(Q_4^2+Q_5^2+Q_6^2)+B_{\alpha\epsilon}\left(\frac{1}{2\sqrt{6}}Q_1Q_3-\frac{1}{2\sqrt{2}}Q_1Q_2\right)$$
$$+B_{\epsilon\epsilon}\left(\frac{1}{4\sqrt{3}}(Q_2^2-Q_3^2)-\tfrac{1}{2}Q_2Q_3\right)+B_{\tau\tau}\tfrac{1}{6}(2Q_4^2-Q_5^2-Q_6^2) ,$$
$$h^q_{22}=A_{\alpha\alpha}\frac{1}{\sqrt{3}}Q_1^2+A_{\epsilon\epsilon}\frac{1}{\sqrt{6}}(Q_2^2+Q_3^2)+A_{\tau\tau}\tfrac{1}{3}(Q_4^2+Q_5^2+Q_6^2)+B_{\alpha\epsilon}\left(\frac{1}{2\sqrt{6}}Q_1Q_3+\frac{1}{2\sqrt{2}}Q_1Q_2\right)$$
$$+B_{\epsilon\epsilon}\left(\frac{1}{4\sqrt{3}}(Q_2^2-Q_3^2)+\tfrac{1}{2}Q_2Q_3\right)+B_{\tau\tau}\tfrac{1}{6}(2Q_5^2-Q_4^2-Q_6^2) ,$$
$$h^q_{33}=A_{\alpha\alpha}\frac{1}{\sqrt{3}}Q_1^2+A_{\epsilon\epsilon}\frac{1}{\sqrt{6}}(Q_2^2+Q_3^2)+A_{\tau\tau}\tfrac{1}{3}(Q_4^2+Q_5^2+Q_6^2)-B_{\alpha\epsilon}\frac{1}{\sqrt{6}}Q_1Q_3$$
$$+B_{\epsilon\epsilon}\frac{1}{2\sqrt{3}}(Q_3^2-Q_2^2)+B_{\tau\tau}\tfrac{1}{6}(2Q_6^2-Q_4^2-Q_5^2) ,$$
$$h^q_{12}=h^q_{21}=-C_{\alpha\tau}\frac{1}{3\sqrt{2}}Q_1Q_6+C_{\epsilon\tau}\frac{1}{3\sqrt{2}}Q_3Q_6+C_{\tau\tau}\tfrac{1}{3}Q_4Q_5 ,$$
$$h^q_{13}=h^q_{31}=-C_{\alpha\tau}\frac{1}{3\sqrt{2}}Q_1Q_5-C_{\epsilon\tau}\left(\frac{1}{2\sqrt{6}}Q_2Q_5+\frac{1}{6\sqrt{2}}Q_3Q_5\right)+C_{\tau\tau}\tfrac{1}{3}Q_4Q_6 ,$$
$$h^q_{23}=h^q_{32}=-C_{\alpha\tau}\frac{1}{3\sqrt{2}}Q_1Q_4+C_{\epsilon\tau}\left(\frac{1}{2\sqrt{6}}Q_2Q_4-\frac{1}{6\sqrt{2}}Q_3Q_4\right)+C_{\tau\tau}\tfrac{1}{3}Q_5Q_6 ,$$

where the A, B, and C's are the linear and quadratic coupling coefficients for the A_{1g}, E_g, and T_{2g} modes, respectively. The above terms in the interaction Hamiltonian were calculated using Griffith's irreducible-tensor method.[17] No spin-orbit interaction was included since the two-electron excited states to be considered are spin-zero states. Also the eight quadratic terms involving the T_{1u} and T_{2u} modes leading to the above symmetries were omitted as these would have doubled the dimensions of the integration and they were not found to be needed.

The calculations are carried out for low temperatures so that A_α is over the zero-point motion only. The nuclear wave function will be the zeroth-order harmonic-oscillator function

$$\chi_{g\alpha}(Q_i)=(\alpha_1\alpha_2\alpha_3/\pi^3)^{1/4}\exp\{-\tfrac{1}{2}[\alpha_1Q_1^2+\alpha_2(Q_2^2+Q_3^2)+\alpha_3(Q_4^2+Q_5^2+Q_6^2)]\} , \quad (5)$$

where $\alpha_i=\mu_i\omega_i/\hbar$. To simplify the numerical calculations, the units of the Q's are chosen such that $\alpha_i=\frac{1}{2}$ and the Gaussian in Eq. (5) has $\sigma=1$. Assuming unpolarized light propagating along the y axis, the dipole-matrix elements in Eq. (1) are proportional to $(a^2+c^2)^{1/2}$ and Eq. (1) reduces to

$$\mu(E)=CE\int\cdots\int dQ_1\cdots dQ_6e^{(-1/2)(Q_1^2+\cdots Q_6^2)}\sum_f(a^2+c^2)_f\delta(E_p+E_{If}-E) . \quad (6)$$

The Gaussian may be eliminated from Eq. (6) by using random values for the Q's having a Gaussian distribution. This greatly reduces the computing time for a given accuracy. The shape function $S(E)=\mu(E)/E$ can then be evaluated using the formula

$$S(E)=C\frac{1}{N_g}\sum_f\sum_{N_g}(a^2+c^2)_f\delta(E_p+E_{If}-E) . \quad (7)$$

The computer program consisted of the following steps. First, random values for the Q's having Gaussian distribution with $\sigma=1$, were generated. Each set of six Q's was then substituted into the interaction matrix which was then numerically diagonalized, resulting in three eigenvalues E_{If} and the a,b,c's for the corresponding eigenfunctions $|f\rangle$. This was repeated N_g times, accumulating $(a^2+c^2)_f$ in energy boxes E_f assigned by $\delta(E_p+E_{If}-E)$. N_g was typically from 10 000 up to 400 000 for the final fitting.

A. T_{2g} as principal interaction mode

Of the three interaction modes, only the T_{2g} is an active mode, that is, a mode that will produce a splitting of the absorption band.[13] While the E_g mode lifts the degeneracy, when the contributions from each of the three states are averaged over a complete period of vibration, a smooth absorption band results with no splitting. Such a mode is called a potentially active mode. Of course the A_{1g} mode alone will not remove the degeneracy although it will produce a Stokes shift. Thus in our initial attempts to find a theoretical fit to the experimental absorption band, we concentrated on T_{2g} as the principal interaction mode.

For reasons that will shortly become apparent, it is desirable to work with the shape function $S(E)$ in this section rather than the absorption coefficient $\mu(E)$. The experimental shape function for the upper LNT curve in Fig. 1 is shown as the smooth curve in Fig. 3 [obtained by dividing $\mu(E)$ by E]. Two features of this curve are to be noted. First, the curve is highly asymmetric with 50% of the area lying to the left of the first minimum at 2 eV. Second, the middle peak at 2.3 eV lies closer to the high-energy peak at 2.8 eV than to the low-energy peak at 1.4 eV.

If only the linear terms are used in the interaction Hamiltonian Eq. (4), and there is no spin-orbit interaction, then in the semiclassical approximation being used here, the shape function

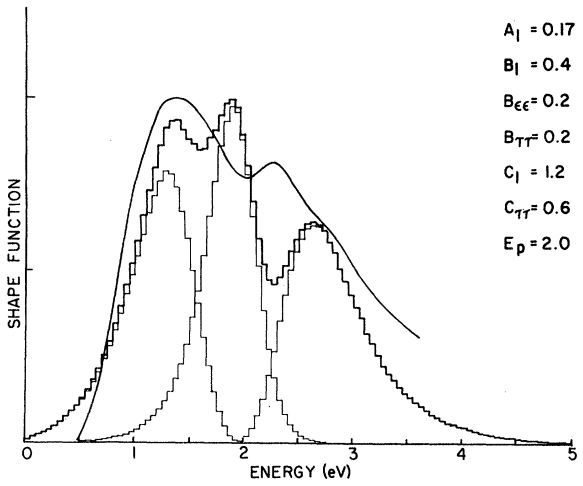

FIG. 3. The smooth curve is the experimental shape function for the F-center optical absorption in BaS. The histogram represents an example of an unsuccessful attempt to fit the data using the T_{2g} modes as the principal modes. Also shown are the histograms for individual contributions of each of the three energy sheets in Q space.

will always be symmetrical.[18] Detailed illustrations of this may be seen in Cho's paper.[4] To introduce asymmetry into the curves it was necessary to include the quadratic terms. However, even with these terms, the degree of asymmetry required to fit the BaS F center could not be obtained. The following argument will prove the impossibility of obtaining a fit to the experimental curve using p-like states alone. Figure 3 shows one such attempt. Again, the smooth curve represents the experimental data and the histogram shows the theoretical curve for the coupling constants indicated. Also shown are the component bands representing the individual contributions from each of the three energy sheets of the excited state in Q space. It was observed and can be proved from symmetry, that the areas under each of these three bands are always equal to each other. Thus it is immediately evident that it will be impossible to obtain 50% of the area under the first peak as required by the experimental curve. The first peak can be increased in amplitude by choosing coupling constants that move the central peak closer, so that more of its low-energy tail will lie under the first peak but the experimental curve shows the central peak to be closer to the high-energy peak. Consequently it was concluded that an additional factor had to be introduced into the theory.

B. T_{2g} mode with perturbing s-like state

One possibility to achieve 50% of the area under the low-energy peak is to split the central peak into two by introducing an additional state. Hopefully then the low-energy half of this peak would combine with the low-energy peak in such a way that a smooth band with no splitting would result. The state chosen was an s-like state $^1S_0[^1A_{1g}]$. This state will not contribute directly to the absorption as transitions to this state are forbidden. But it will mix with the nearby p-like states, displacing them so as to alter the structure of the shape function.

The new interaction Hamiltonian will now be a 4×4 matrix and the eigenfunctions will be of the form

$$|f\rangle = a|x\rangle + b|y\rangle + c|z\rangle + d|s\rangle \ . \tag{8}$$

The symmetries of the vibrational modes that will mix the s-like states with the p-like states are given by the direct product $[A_{1g}\times T_{1u}]=T_{1u}$. Again following Sturge,[14] there are two kinds of T_{1u} modes, (Q_7,Q_8,Q_9) and (Q_{10},Q_{11},Q_{12}). We use a linear combination of these to preserve the center of gravity and call these linear combinations Q_7, Q_8, and Q_9. The additional linear terms in the interaction Hamiltonian were found to be

$$h^1_{14} = h^1_{41} = F_1 Q_7 / 3^{1/2} ,$$
$$h^1_{24} = h^1_{42} = F_1 Q_8 / 3^{1/2} , \quad (9)$$
$$h^1_{34} = h^1_{43} = F_1 Q_9 / 3^{1/2} ,$$
$$h^1_{44} = G_1 Q_1 + E_s ,$$

where F_1 is the linear coupling constant that mixes the s-like states with the p-like states, G_1 is the linear coupling constant that mixes the s-like state with itself, and E_s is the displacement of the unperturbed s-like state from the unperturbed p-like state. Here again, the five additional quadratic terms leading to T_{1u} symmetry involving the T_{1u} and T_{2u} modes have been omitted.

Since the now four component bands due to the contributions from the now four energy sheets in Q space no longer have equal areas and since the three peaks in the experimental curves are more clearly distinguishable in the absorption curve, it will be more convenient to work with the absorption coefficient $\mu(E)$ from here on. The best fit using T_{2g} as the principal mode resulted in the size of the three peaks being about right but the middle peak was shifted to too low an energy, it being almost exactly midway between the other two peaks. The parameters for this fit were $A_1 = 0.5$, $B_1 = 0.1$, $C_1 = 1.3$, $F_1 = 0.5$, $A_{\epsilon\epsilon} = 0.1$, $B_{\tau\tau} = 0.5$, $C_{\tau\tau} = 0.8$, $E_p = 1.9$, and $E_s = 0.1$. As will be discussed in the next section, a much better fit was obtained using E_g as the principal mode.

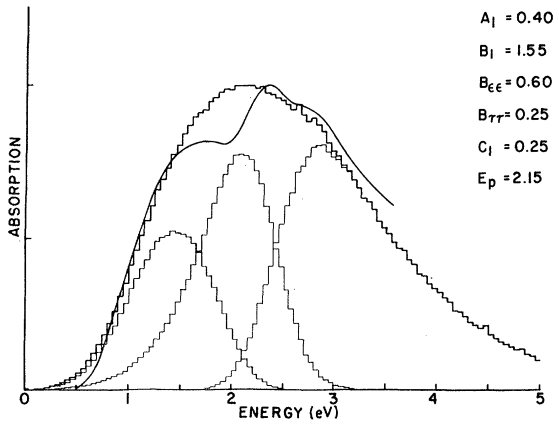

FIG. 4. The smooth curve is the experimental optical absorption due to the F center in BaS. The histogram is the theoretical optical absorption when only E_g mode is used, illustrating how the contributions from the three energy sheets in Q space combine to produce a smooth bell-shaped curve. The parameters are the same as used in Fig. 5 except that the s state has been omitted.

C. E_g mode with perturbing s-like state

As mentioned earlier, the E_g mode is a potentially active mode. That is, when it is the principal mode, it will give rise to instantaneous level splittings but will not give rise to absorption-band splitting, even when the quadratic terms are included. This is illustrated in Fig. 4. However, as will now be shown, when a nearby s-like state is introduced, the resulting perturbation changes this.

Choosing the E_g mode as the principal mode and positioning the s-like state to split the central band, values for the coupling constants were found which resulted in a very good fit to the experimental data. This fit is shown in Fig. 5. The unperturbed p-like state was taken at $E_p = 2.15$ eV with the s-like state below it by $E_s = -0.05$ eV. The coupling coefficients which significantly differed from zero were $A_1 = 0.4$, $B_1 = 1.55$, $C_1 = 0.25$, $F_1 = 0.45$, $G_1 = 0.07$, $B_{\epsilon\epsilon} = 0.6$, and $B_{\tau\tau} = 0.25$. The accuracy of the coupling constants is estimated to be about 0.05 units. That is, changes of this magnitude produce changes in the histogram comparable with the changes resulting from different sets of random numbers. Figure 5 was the result of using 400 000 points in Q space which required about 16 min. of CPU time on the Amdahl 470/V7 computer.

It should be stressed at this point that the observed splitting of the F band in BaS is not so much a result of a large Jahn-Teller interaction as it is a consequence of the p-like states being perturbed by the nearby s-like state. As was illustrated in Fig. 4, F centers in general could have, and probably do have, a large Jahn-Teller

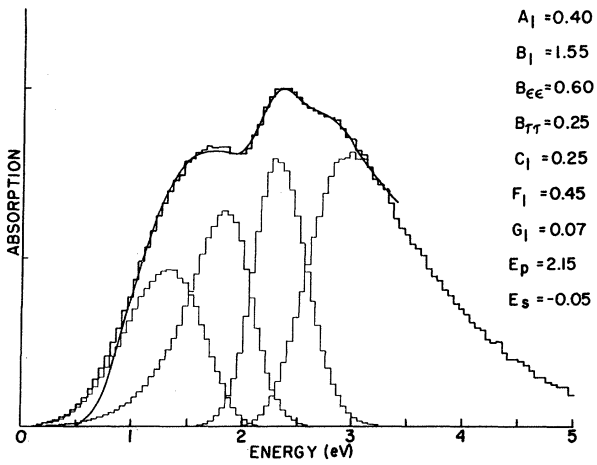

FIG. 5. Best fit of the theory to the experimental optical absorption of the F center in BaS using the indicated parameters.

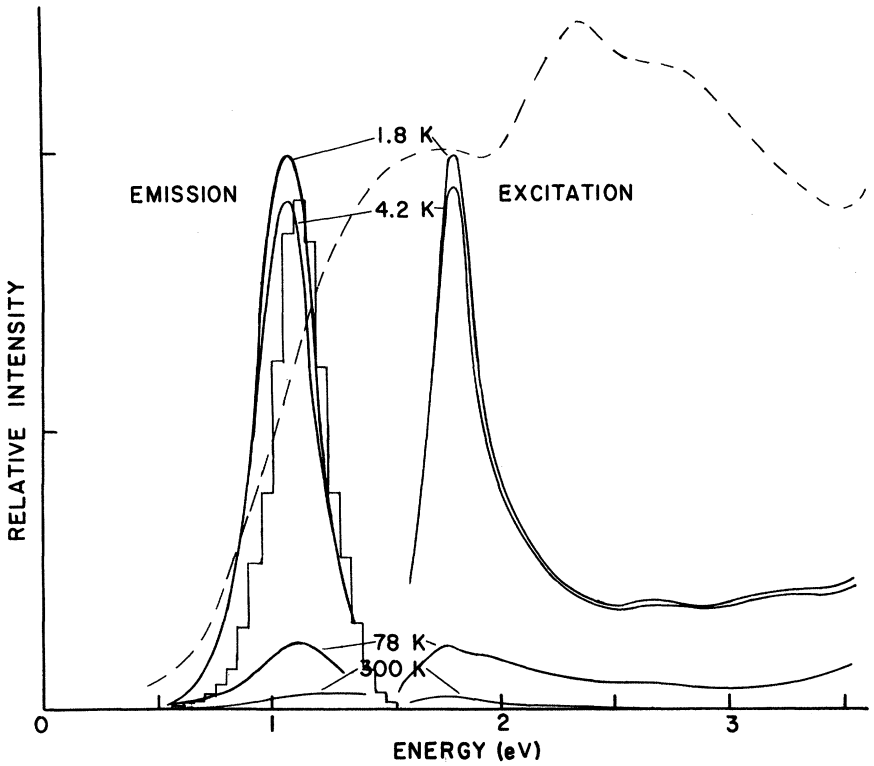

FIG. 6. Luminescence spectra and corresponding excitation spectra observed from additively colored BaS crystal at four different temperatures. For comparison, the optical absorption of the F center in BaS is shown by the broken curve. The histogram shows the predicted luminescence using the same parameters as in Fig. 5 but with an unrealistic value for $E_{0i}=0.4$ eV. It was concluded that the observed luminescence was *not* due to the F center.

interaction due to E_g modes and yet usually will not display any splitting of the F band.

IV. LUMINESCENCE

An attempt was made to observe luminescence from the F centers in BaS. A luminescence spectrum was observed. However, based on our calculations, we have concluded that it must be due to an impurity and that in fact no luminescence from the F center is to be expected.

Experimentally, light from a 1000-watt xenon lamp was passed through a Bausch and Lomb model 33-86-02 grating monochromator and a Schott KG1 high pass filter and focused onto the BaS crystal mounted in a liquid-helium Dewar. The emission was focused by a system of spherical mirrors and passed through a 700-hertz light chopper, a Wratten 87C low pass filter, and a Perkin-Elmer model 83 NaCl prism monochromator. The output was detected by a PbS detector using a lock-in amplifier.

In only one crystal could any luminescence be observed at temperatures higher that LNT. Figure 6 shows the observed emission spectra for this crystal at several temperatures along with the corresponding excitation spectra. This crystal had a density of F centers of $1.35\times10^{17}\,\mathrm{cm}^{-3}$. A similar luminescence was also observed in two other crystals having F-center densities of 5.78×10^{17} and $13.1\times10^{17}\,\mathrm{cm}^{-3}$ but the emission intensities were reduced relative to the first crystal by factors of 1.2×10^{-3} and 1.2×10^{-4}, respectively.

A calculation of the possibility of luminescence in the presence of a strong Jahn-Teller interaction using Monte Carlo integration will be described with the aid of Fig. 7. This figure shows a cross section of the energy surfaces in Q space along the Q_3 coordinate using the same parameters as were used for Fig. 5. The ground state was plotted using the equation

$$V_g=\alpha_1E_{01}Q_1^2+\alpha_2E_{01}(Q_2^2+Q_3^2)+\alpha_3E_{03}(Q_4^2+Q_5^2+Q_6^2)+\alpha_4E_{04}(Q_7^2+Q_8^2+Q_9^2)\,, \tag{10}$$

and the excited states using the equation

$$V_f=V_g+E_p+E_{If}(Q_1\cdots Q_9)\,. \tag{11}$$

For Fig. 7, the zero-point energies $E_{0i}=\frac{1}{2}\hbar\omega_i$ were given a value of 0.4 eV, the lowest value that would result in definite minima in the lowest-energy sheet from which luminescence could

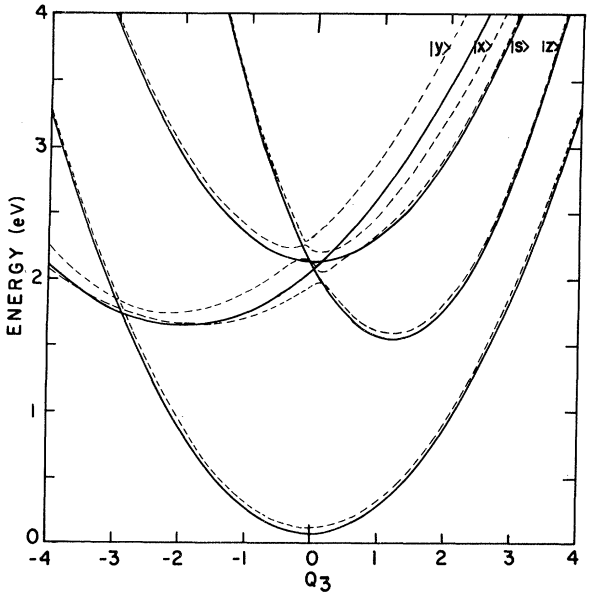

FIG. 7. Cross sections of the energy surfaces in Q space along Q_3 coordinate using same parameters as for Fig. 5 and with $E_{0i}=0.4$ eV. Solid curves are for $Q_1=-0.58$ and all other Q's set equal to zero. The broken curves are for all these other Q's set equal to 0.2.

occur. Similar plots for the other Q's show these absolute minima to be at $Q_1=-0.57$, $(Q_2, Q_3)=(0, 1.20)$, $(0.60, -1.04)$, $(-0,60, -1.04)$, and $Q_4, \ldots, Q_9=0.0$. Electrons excited to the upper-energy sheets will decay in times short compared with the dipole emission lifetime. Most of these will reach the ground state via the intersections between V_g and the two lower-energy surfaces as seen at about $Q_3=-2.9$ in Fig. 7. However some of the electrons will come to quasiequilibrium in the lowest-energy state determined by the minima in the lowest-energy sheet. These electrons will then have time to make radiative transitions to the ground state. It may be noted that such a sequence could qualitatively explain the shape of the excitation spectra in Fig. 6.

Derivation of the expression for the emission spectra is similar to that for Eq. (1) except that the photon energy E appears raised to the third power [see Dexter, Eq. (7.8)].[15] The corresponding expression for the Monte Carlo integration is

$$I(E)=C'E^3\frac{1}{N}\sum_f\sum_N (a^2+b^2)_f\, e^{-(V_f-V_m)/V_0} \times\delta(E_p+E_{If}-E). \quad (12)$$

In this expression, the square of the wave function is expressed by the quasi-Boltzmann factor in which V_m is the absolute minimum of the potential energy for the excited state, and the zero-point energy V_0 is used in place of kT. Note that if V_g with E_{0i}'s $=V_0$ and $\alpha_i=\frac{1}{2}$ is substituted in place of V_f and $V_m=0$, then the Gaussian wave function used in Eq. (6) will be recovered. Since the exponential in Eq. (12) is no longer a Gaussian, it is necessary to carry out the Monte Carlo integration using uniformly distributed random numbers.

The histogram in Fig. 6 shows the luminescence predicted by this model using the same parameters as were used for Fig. 5, $V_0=0.03$ eV and E_{0i}'s $=0.4$ eV. Reducing $B_{\epsilon\epsilon}$ to 0.5 would shift the peak downward into good agreement with the observed peak; however, this discrepancy is minor compared with the completely unacceptable value for the zero-point energies $E_{0i}=0.4$ eV. This value for the E_{0i}'s is also quite different from the more reasonable value for $V_0=0.03$ eV but is the smallest value which would result in a definite minimum in the lowest-energy sheet in Fig. 7. Note that the absorption calculation was not dependent on the values for the E_{0i}'s.

Figure 8 shows the potential-energy curves for a more reasonable value for the zero-point energies $E_{0i}=0.03$ eV. Note that no minima are present. The apparent minimum at $Q_3=2.3$ is actually a saddle point as the surface bends downward in both Q_2 directions. From this we concluded that luminescence from the $^1P_1$ state will not be possible when the Jahn-Teller interaction is much stronger than the zero-point energy. There re-

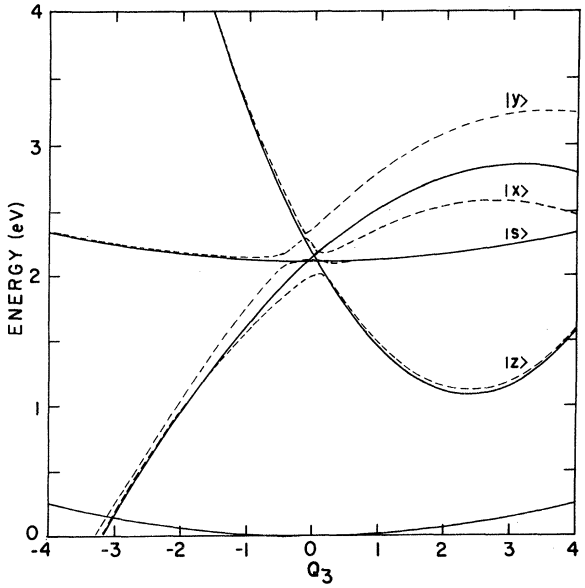

FIG. 8. Cross sections of the energy surfaces in Q space along the Q_3 coordinate using same parameters as for Fig. 5 but with $E_{0i}=0.03$ eV. Solid curves are for all other Q's equal to zero and broken curves are for all other Q's equal to 0.2.

mains the possibility of other states lying below the $^1P_1$ state such as the ^3P or ^3S. The ^3P states are unlikely candidates as they would be expected to experience essentially the same Jahn-Teller interactions as the $^1P_1$ state and with similar results. However the possibility that the luminescence originates from a ^3S state is intriguing as examination of Fig. 8 shows ample room for such a state about 1.1 eV above the ground state (the classical turning points would be about 2 units apart for the scale used). Thus direct transitions to and from the ground state together with a modest Stokes shift due to the A_{1g} mode could easily account for the shape of both the emission peak and the principal peak in the excitation spectra. The high-energy tail in the excitation spectra would result from electrons leaking from the $^1P_1$ state into the ^3S state. However, not only are the $^3S \rightarrow {}^1S$ transitions both parity and spin forbidden, but calculations show that the inclusion of this ^3S state in the interaction Hamiltonian with coupling coefficients comparable with those used for the upper ^1S state will result in pronounced structure in the low-energy tail of the absorption which was not observed. Consequently we conclude that the observed luminescence is most probably due to an unknown impurity.

ACKNOWLEDGMENTS

The authors are grateful to Professor David Cowan for the many helpful discussions throughout the course of this investigation. We also wish to thank Frank S. Ham for some very constructive comments which lead to substantial improvements in this paper. This work was supported in part by the National Science Foundation.

---

*Permanent address: Dept. of Physics, Lincoln University, Jefferson City, Mo. 65101.

[1]H. E. Hughes and B. Henderson, in *Defects in Crystalline Solids*, edited by J. H. Crawford and L. M. Slifkin (Plenum, New York, 1972).

[2]J. L. Kolopus and G. J. Lapeyre, Phys. Rev. 176, 1025 (1968).

[3]Strickly speaking, in this paper we are considering only the Jahn-Teller interaction and not the Jahn-Teller effect since the degeneracy is in the excited state. This is frequently referred to in the literature as the dynamical Jahn-Teller effect, however, it should be distinguished from the situation where the Jahn-Teller energy is comparable to the zero-point phonon energy which is the more common meaning of the dynamic Jahn-Teller effect. In this latter sense, we are clearly dealing with the static Jahn-Teller effect in this investigation as is indicated by the very large splitting of the peaks in our absorption spectra.

[4]K. Cho, J. Phys. Soc. Jpn. 25, 1372 (1968).

[5]C. H. Henry and C. P. Slichter, in *Physics of Color Centers*, edited by W. B. Fowler (Academic, New York, 1968), Chap. 6, p. 351.

[6]R. B. Reed, J. Appl. Phys. 32, 2534 (1961).

[7]The crystals were analyzed for impurities using both activation analysis and flame spectroscopy. Approximately 100-ppm Al was found with smaller amounts of Si and Cu and somewhat larger amounts of the other alkaline earths. No evidence of these impurities could be detected in the optical-absorption spectra. Since the Al content was observed to be greatly reduced by the crystallization process, it is probable that the remaining amounts detected are concentrated primarily in crystal defects, such as dislocations.

[8]E. B. Hensley, W. C. Ward, B. Johnson, and R. L. Kroes, Phys. Rev. 175, 1223 (1968).

[9]J. D. Foster and E. B. Hensley, Phys. Rev. B 11, 3966 (1975).

[10]A. N. Nesmeyanov, in *Vapor Pressure of the Elements*, translated and edited by J. I. Carass (Academic, New York, 1963), p. 443.

[11]D. L. Dexter, Phys. Rev. 101, 48 (1956).

[12]*Handbook of Chemistry and Physics*, edited by R. C. Weast (Chemical Rubber Co., Cleveland, 1969), p. B-91.

[13]Y. Toyozawa and M. Inoue, J. Phys. Soc. Jpn. 21, 1663 (1966).

[14]M. D. Sturge, Solid State Phys. 20, 91 (1967).

[15]D. L. Dexter, Solid State Phys. 6, 353 (1958).

[16]In a limited sense it could be argued that we are still making the Condon approximation in that we continue to assume that the radial part of the wave function is independent of the nuclear coordinates. Also this procedure is nonessential at this point since it can be shown that the average of the matrix element over the equivalent distortions of the cubic group is independent of both the Q's and the eigenvalues of H_I. However, when a nondegenerate state is allowed to mix with the degenerate excited state, this is no longer true and the matrix element must be left inside the integral.

[17]J. S. Griffith, *The Irreducible Tensor Method for Molecular Symmetry Groups* (Prentice Hall, New Jersey, 1962).

[18]This will not be true for the dynamic Jahn-Teller effect (see Ref. 3) since the inclusion of the nuclear kinetic-energy operators in the Hamiltonian will result in an asymmetric broadening of the shape function as has been shown by Englman, Caner, and Toaff, J. Phys. Soc. Jpn. 29, 306 (1980). Note that the bands in the Englman paper are very narrow compared with the the *F* band in BaS.